The Triphenylphosphine Cone Angle and Restricted Rotation about the Chromium–Phosphorus Bond in Dicarbonyl(η^6-hexa-alkylbenzene)(triphenylphosphine)chromium(0) Complexes. Crystal and Molecular Structure† of Dicarbonyl(η^6-hexa-n-propylbenzene)(triphenylphosphine)chromium(0)

Geoffrey Hunter* and Timothy J. R. Weakley
Department of Chemistry, The University, Dundee DD1 4HN
Walter Weissensteiner
Institut für Organische Chemie, Universität Wien, A-1090 Wien, Austria

The variable-temperature 90.56-MHz ^{13}C-{^1H} n.m.r. spectra of dicarbonyl(η^6-benzene)(triphenylphosphine)chromium(0), (**1**), dicarbonyl(η^6-hexamethylbenzene)(triphenylphosphine)chromium(0), (**2**), dicarbonyl(η^6-hexaethylbenzene)(triphenylphosphine)chromium(0), (**3**), and dicarbonyl(η^6-hexa-n-propylbenzene)(triphenylphosphine)chromium(0), (**4**), have been observed and a decoalescence in the triphenylphosphine subspectra of (**2**), (**3**), and (**4**), with $\Delta G_{200}^{\ddagger}$ *ca.* 38 kJ mol^{-1}, attributed to restricted rotation about the chromium–phosphorus bond. The steric requirements for intramolecular rotations for these complexes are visualised as two cones with a common apex at the centre of the chromium atom. The crystal and molecular structure of (**4**) has been determined and the co-ordinated hexa-n-propylbenzene has been found to adopt an all-distal alkyl group conformation.

This paper reports the results of a variable-temperature n.m.r. study whose aim was to quantify the effect induced by the alkyl substituents of homosubstituted hexa-alkylbenzenes, C_6R_6, on the barrier to rotation about the chromium–phosphorus bond axis in the series of complexes [$Cr(\eta^6\text{-}C_6R_6)(CO)_2(PPh_3)$] [R = H (**1**), Me (**2**), Et (**3**), or Pr^n (**4**)]. The single-crystal *X*-ray structure of (**4**) is also reported. We find that even the otherwise stereochemically-inactive methyl groups of hexamethylbenzene can cause observable stereodynamical effects elsewhere within a complex molecule. Our previous view has been that hexaethylbenzene is the smallest homosubstituted hexa-alkylbenzene in which are manifested the effects of steric overcrowding and in which the size and orientation of the alkyl groups relative to the benzene ring plane have major influence on the stereochemistry and stereodynamics of a transition metal π-complex.[1]

There are relatively few reports of measured barriers to rotation about a metal–phosphorus bond and almost all of these are for complexes of phosphines with platinum-group metals.[2] An exception is the barrier to rotation about the Fe–P bond in [$Fe(\eta^5\text{-}C_5H_5)(CO)(CN)(PR'_3)$] complexes which, despite the absence of decoalescence phenomena in the ^{13}C n.m.r. spectra, has been estimated to be less than 32 kJ mol^{-1}.[3] What is apparent from the published data is that steric, rather than electronic, factors are dominant in determining actual barriers to rotation about a metal–phosphorus bond.

Results and Discussion

Static Stereochemistry.—Empirical force field calculations, details of which will be reported elsewhere, indicate that the free hexa-n-propylbenzene molecule adopts a D_{3d} ground state and that the stereoisomer of highest energy (39 kJ mol^{-1} relative to the ground state) is the one with all six pendant alkyl groups on the same side of the benzene ring, with C_6 rather than C_{6v} symmetry. All stereoisomers have their terminal methyl groups extending outwards from the core of the molecule, so attractive van der Waals forces are not important in stabilizing any conformation of $C_6Pr^n_6$. When $C_6Pr^n_6$ acts as a hexahapto ligand, however, the stereochemistry it adopts is the result of a balance of repulsive steric interactions, those arising within the arene among the alkyl groups and those between the alkyl groups and other ligands bound to the metal.

In (**4**) the $C_6Pr^n_6$ stereoisomer is that of highest energy for the free ligand, with all six alkyl groups fully extended and orientated distally with respect to the chromium atom (Figure 1). The effect of the bulky PPh_3 ligand on $C_6Pr^n_6$ in (**4**) i. thus very similar to its effect on C_6Et_6 in (**3**), whose structure[1b] is shown for comparison in Figure 2. Other similar features of (**3**) and (**4**) are (*i*) the staggered conformations with respect to the Cr–P bonds [Figures 1(*a*) and 2(*a*)]; (*ii*) the similar tilt angles [(**3**), 2.5; (**4**), 2.6°] between the normal to the arene ring plane and the line Cr–c(0) [c(0) = ring centroid]; (*iii*) similar P–Cr–c(0) angles [(**3**), 132.8; (**4**), 132.4°]; (*iv*) similar staggered conformations about the Cr–c(0) axis [(**4**), Figure 3] such that the carbonyl ligands do not eclipse the alkyl groups; and (*v*) evidence from the C–P–C angles of some strain in the PPh_3 ligand [(**3**), 97.5, 101.5, 104.1; (**4**), 97.0, 103.1, 105.6; non-co-ordinated PPh_3,[4] 103°]. As in the case of (**3**) the individual C–C bond lengths in the arene ring vary considerably (Table 1), although the average value in each compound [(**3**), 1.424; (**4**), 1.426 Å] is not significantly different from that found for [$Cr(\eta^6\text{-}C_6Et_6)(CO)_3$][1b] (1.421 Å).

The crystal structures of (**1**) and (**2**) are unknown but it is plausible that these molecules also have staggered conformations about the P–Cr bonds and that, as in (**3**) and (**4**) [Figures 1(*b*) and 2(*b*)], one of the phenyl rings is remote from, and the other two are closer to, the steric and electronic influences of the η^6-arene ligand.

Variable-temperature N.M.R. Spectra.—Solutions of the complexes in CD_2Cl_2 were cooled to 158 K and their 90.56-MHz ^{13}C-{^1H} n.m.r. spectra recorded. No decoalescence phenomena were revealed in the alkyl, hexahapto arene, or carbonyl subspectra of any of the complexes indicating that (*i*) rotation about the chromium–arene bond axis remains rapid even at the lowest temperatures observed, and (*ii*) in (**3**) and (**4**)

† *Supplementary data available:* see Instructions for Authors, *J. Chem. Soc., Dalton Trans.*, 1987, Issue 1, pp. xvii—xx.

Non-S.I. unit employed: Torr ≈ 133 Pa.

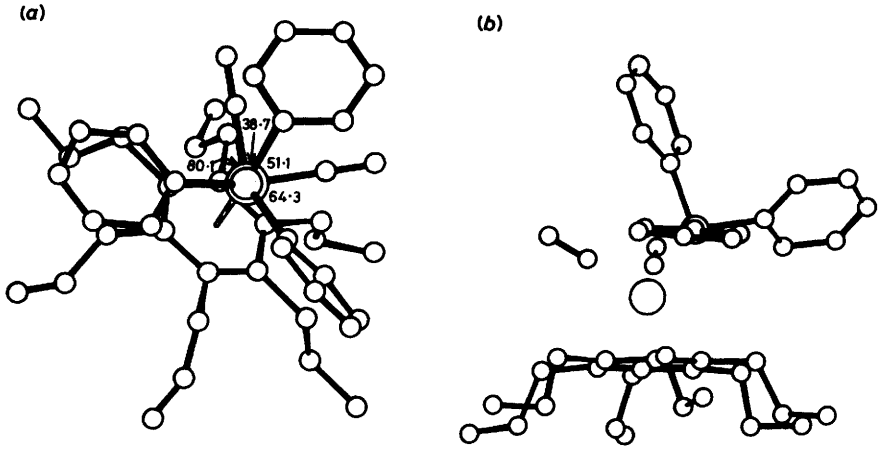

Figure 1. The molecular structure of (**4**) viewed along (*a*) the chromium–phosphorus bond axis, with torsion angles; (*b*) one of the carbon–phosphorus bond axes

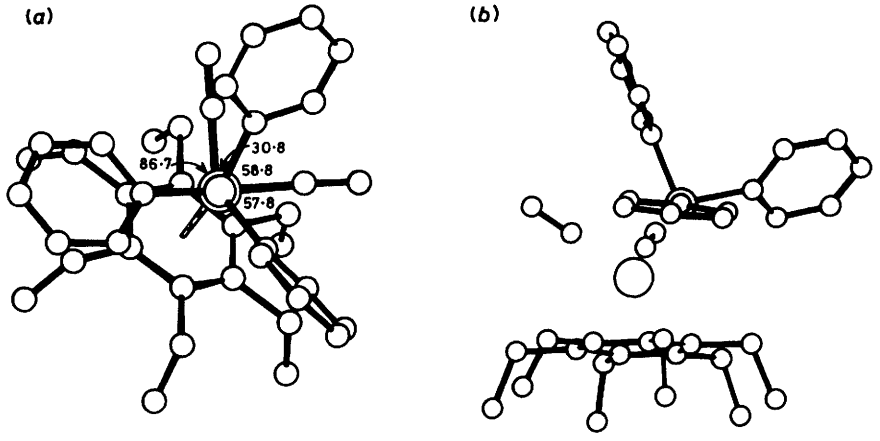

Figure 2. The molecular structure of (**3**) viewed along (*a*) the chromium–phosphorus bond axis, with torsion angles; (*b*) one of the carbon–phosphorus bond axes

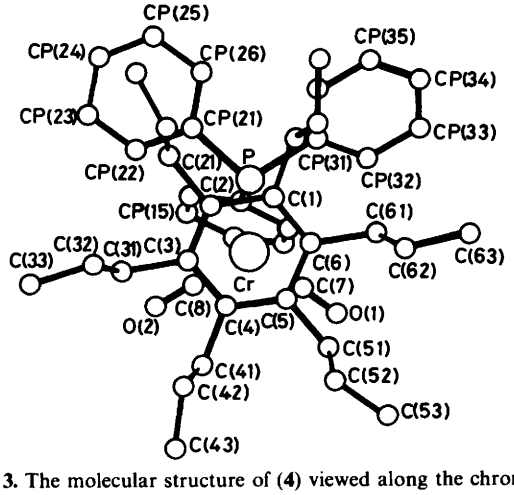

Figure 3. The molecular structure of (**4**) viewed along the chromium–arene bond axis

the hexa-alkylbenzene stereoisomers with all the alkyl groups distal to the chromium atom, as observed in their crystal structures, are retained in solution. However, a decoalescence phenomenon in the triphenylphosphine subspectrum was observed for (**2**), (**3**), and (**4**), but not for (**1**). The intramolecular origin of this decoalescence was confirmed by observation, in the ambient-temperature ^{13}C-{^1H} and 145.87-MHz ^{31}P-{^1H} spectra, of separate signals for the complexes and triphenylphosphine which had been added to their solutions. The 90.56-MHz ^{13}C-{^1H} triphenylphosphine subspectrum of (**2**) in CD_2Cl_2 at 168 K is illustrated in Figure 4. N.m.r. data for the complexes are reported in Table 2. In the ambient-temperature spectra, the relative magnitudes of J_{PC} (Hz) were used to assign signals to the individual carbon atoms of the complexed triphenylphosphine moiety: *ipso*, $^1J_{PC}$ *ca.* 30; *ortho*, $^2J_{PC}$ *ca.* 11; *meta*, $^3J_{PC}$ *ca.* 8.[3] No splitting due to $^4J_{PC}$ was observed for those signals assigned to the *para* carbon atoms. Application of the DEPT pulse sequence caused the disappearance of those signals assigned to the *i*-C atoms, thus confirming their correct assignment.

Below the coalescence temperature for each complex, the signals assigned to *i*-C and *o*-C atoms each separate into two components of approximate intensity ratio 1:2. For (**2**) and (**4**), the signal arising from the *p*-C atoms also shows a similar decoalescence. For the decoalesced signals of the *i*-C atoms, whose correct assignment was once again confirmed by their disappearance on application of the DEPT pulse sequence, the doublet splittings resulting from spin–spin coupling with the phosphorus atom are well resolved and it is noteworthy that for

Table 1. Bond distances (Å) and angles (°) for (4)*

C(1)–Cr	2.266(7)	C(4)–C(3)	1.424(9)	C(33)–C(32)	1.535(12)	CP(15)–CP(14)	1.362(13)
C(2)–Cr	2.280(6)	C(31)–C(3)	1.555(10)	C(42)–C(41)	1.543(9)	CP(16)–CP(15)	1.392(13)
C(3)–Cr	2.247(6)	C(5)–C(4)	1.430(9)	C(43)–C(42)	1.519(13)	CP(22)–CP(21)	1.433(12)
C(4)–Cr	2.192(6)	C(41)–C(4)	1.532(11)	C(52)–C(51)	1.525(9)	CP(26)–CP(21)	1.389(13)
C(5)–Cr	2.188(6)	C(6)–C(5)	1.438(11)	C(53)–C(52)	1.500(10)	CP(23)–CP(22)	1.402(10)
C(6)–Cr	2.264(7)	C(51)–C(5)	1.521(9)	C(62)–C(61)	1.499(9)	CP(24)–CP(23)	1.395(19)
C(7)–Cr	1.833(6)	C(61)–C(6)	1.555(9)	C(63)–C(62)	1.563(12)	CP(25)–CP(24)	1.363(19)
C(8)–Cr	1.816(9)	O(1)–C(7)	1.170(8)	CP(11)–P	1.849(7)	CP(26)–CP(25)	1.418(13)
c(0)–Cr	1.726(9)	O(2)–C(8)	1.156(11)	CP(21)–P	1.841(7)	CP(32)–CP(31)	1.389(10)
P–Cr	2.305(2)	C(12)–C(11)	1.510(10)	CP(31)–P	1.845(8)	CP(36)–CP(31)	1.412(11)
C(2)–C(1)	1.449(9)	C(13)–C(12)	1.542(15)	CP(12)–CP(11)	1.348(10)	CP(33)–CP(32)	1.420(12)
C(6)–C(1)	1.412(9)	C(22)–C(21)	1.555(10)	CP(16)–CP(11)	1.360(11)	CP(34)–CP(33)	1.371(12)
C(11)–C(1)	1.497(11)	C(23)–C(22)	1.486(13)	CP(13)–CP(12)	1.405(10)	CP(35)–CP(34)	1.362(14)
C(3)–C(2)	1.401(11)	C(32)–C(31)	1.523(10)	CP(14)–CP(13)	1.329(13)	CP(36)–CP(35)	1.388(13)
C(21)–C(2)	1.532(9)						
C(8)–Cr–C(7)	89.8(3)	C(51)–C(5)–C(4)	122.0(7)	C(62)–C(61)–C(6)	114.7(5)	CP(22)–CP(21)–P	116.4(6)
P–Cr–C(7)	88.0(2)	C(51)–C(5)–C(6)	118.1(6)	C(63)–C(62)–C(61)	108.8(6)	CP(26)–CP(21)–P	124.5(6)
P–Cr–C(8)	87.8(2)	C(5)–C(6)–C(1)	118.7(6)	CP(11)–P–Cr	115.6(2)	CP(26)–CP(21)–CP(22)	118.8(7)
P–Cr–c(0)	132.4(7)	C(61)–C(6)–C(1)	120.2(6)	CP(21)–P–Cr	113.5(2)	CP(23)–CP(22)–CP(21)	122.0(9)
C(6)–C(1)–C(2)	120.6(7)	C(61)–C(6)–C(5)	121.1(6)	CP(21)–P–CP(11)	103.1(3)	CP(24)–CP(23)–CP(22)	117.1(9)
C(11)–C(1)–C(2)	119.2(6)	O(1)–C(7)–Cr	175.8(5)	CP(31)–P–Cr	119.7(2)	CP(25)–CP(24)–CP(23)	121.9(9)
C(11)–C(1)–C(6)	120.1(6)	O(2)–C(8)–Cr	178.5(6)	CP(31)–P–CP(11)	97.0(3)	CP(26)–CP(25)–CP(24)	121.7(12)
C(3)–C(2)–C(1)	120.6(6)	C(12)–C(11)–C(1)	114.1(6)	CP(31)–P–CP(21)	105.6(4)	CP(25)–CP(26)–CP(21)	118.4(9)
C(21)–C(2)–C(1)	120.7(7)	C(13)–C(12)–C(11)	111.5(7)	CP(12)–CP(11)–P	117.2(5)	CP(32)–CP(31)–P	118.9(6)
C(21)–C(2)–C(3)	118.6(6)	C(22)–C(21)–C(2)	114.3(5)	CP(16)–CP(11)–P	123.8(5)	CP(36)–CP(31)–P	122.9(6)
C(4)–C(3)–C(2)	119.0(6)	C(23)–C(22)–C(21)	110.3(6)	CP(16)–CP(11)–CP(12)	118.9(7)	CP(36)–CP(31)–CP(32)	118.1(7)
C(31)–C(3)–C(2)	122.4(6)	C(32)–C(31)–C(3)	114.0(6	CP(13)–CP(12)–CP(11)	120.8(7)	CP(33)–CP(32)–CP(31)	121.8(7)
C(31)–C(3)–C(4)	118.6(7)	C(33)–C(32)–C(31)	112.8(7)	CP(14)–CP(13)–CP(12)	118.6(7)	CP(34)–CP(33)–CP(32)	118.2(8)
C(5)–C(4)–C(3)	121.0(7)	C(42)–C(41)–C(4)	112.5(6)	CP(15)–CP(14)–CP(13)	121.8(9)	CP(35)–CP(34)–CP(33)	120.6(9)
C(41)–C(4)–C(3)	120.8(6)	C(43)–C(42)–C(41)	111.8(7)	CP(16)–CP(15)–CP(14)	120.1(9)	CP(36)–CP(35)–CP(34)	122.3(8)
C(41)–C(4)–C(5)	118.2(6)	C(52)–C(51)–C(5)	115.2(5)	CP(15)–CP(16)–CP(11)	119.7(8)	CP(35)–CP(36)–CP(31)	118.9(7)
C(6)–C(5)–C(4)	119.9(6)	C(53)–C(52)–C(51)	111.8(6)				

* c(0) is the centroid of the arene ring.

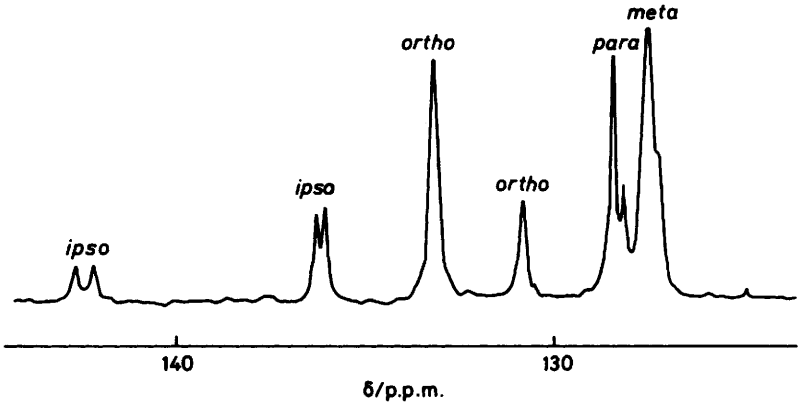

Figure 4. The 90.56-MHz ^{13}C-{^{1}H} triphenylphosphine subspectrum of (2) in CD_2Cl_2 at 168 K

all three complexes this coupling is considerably greater for the less intense downfield signal. For each complex, the mean value of $^{1}J_{PC}$ for the upfield and downfield components approximates closely to that observed for the coalesced *i*-C signal at ambient temperature. Although below decoalescence there was some evidence of fine structure on the signals assigned to the *o*-C and *m*-C atoms, this could not reliably be assigned to phosphorus–carbon coupling.

Only two slowed intramolecular exchange processes can conceivably account for decoalescence phenomena observed in the triphenylphosphine subspectrum: (*i*) rotation about the phenyl *i*-C–P bond, and (*ii*) rotation about the Cr–P bond. By itself process (*i*) cannot lead to separate environments for the *i*-C atoms of the three phenyl rings and can therefore be discounted. Moreover, at the lowest temperature observed there was no evidence of any decoalescence of the carbonyl signal nor of any further decoalescence involving the signals of the phenyl *o*-C and *m*-C atoms, indicating that on the time-scale of observation there is both mirror symmetry for the molecule and rapid rotation about the C–P bonds. The observed decoalescence phenomenon can therefore unequivocally be attributed to slowed rotation about the Cr–P bond, with all other possible intramolecular rotations remaining rapid. If it is assumed that the staggered conformation about the Cr–P bond observed in

Table 2. $^{13}C-\{^1H\}$ N.m.r. data for the complexes (δ values, J_{PC} in Hz)

Complex	Temperature	C_{alkyl}	C_{arene}	CO	*i*-C	*o*-C	*m*-C	*p*-C
(1)	Ambient		89.82	240.63 (17.6)[a]	138.29 (33.7)[b]	132.04 (10.9)[c]	127.24 (8.0)[d]	128.30
(2)	Ambient	15.60	101.66	242.84 (21.2)[a]	138.81 (30.0)[b]	132.58 (11.0)[c]	126.96 (8.1)[d]	127.82
	158 K				142.23[f] (43.8)[b]	132.85[e]	127.17[g]	128.13[e]
					136.10[e] (19.9)[b]	130.60[f]		127.86[f]
(3)	Ambient	23.04 (CH_2)	108.98	243.84 (22.0)[a]	139.90 (29.6)[b]	133.40 (10.6)[c]	127.63 (8.0)[d]	128.53
		16.60 (CH_3)						
	158 K				142.05[f] (45.8)[e]	132.84[e]	127.16	128.06
					136.56[e] (21.5)[b]	130.48[f]		
(4)	Ambient	32.69 (CH_2)	107.51	243,42 (21.5)[a]	139.10 (31.6)[b]	132.90 (10.8)[c]	127.52 (8.0)[d]	128.10
		24.61 (CH_2)						
		14.67 (CH_3)						
	158 K				142.53[f] (50.8)[b]	133.59[e]	127.65	128.69[e]
					136.69[e] (22.0)[b]	131.07[f]		128.39[f]

[a] ($^2J_{PC}$). [b] ($^1J_{PC}$). [c] ($^2J_{PC}$). [d] ($^3J_{PC}$). [e] More intense component. [f] Less intense component. [g] Plus upfield shoulder.

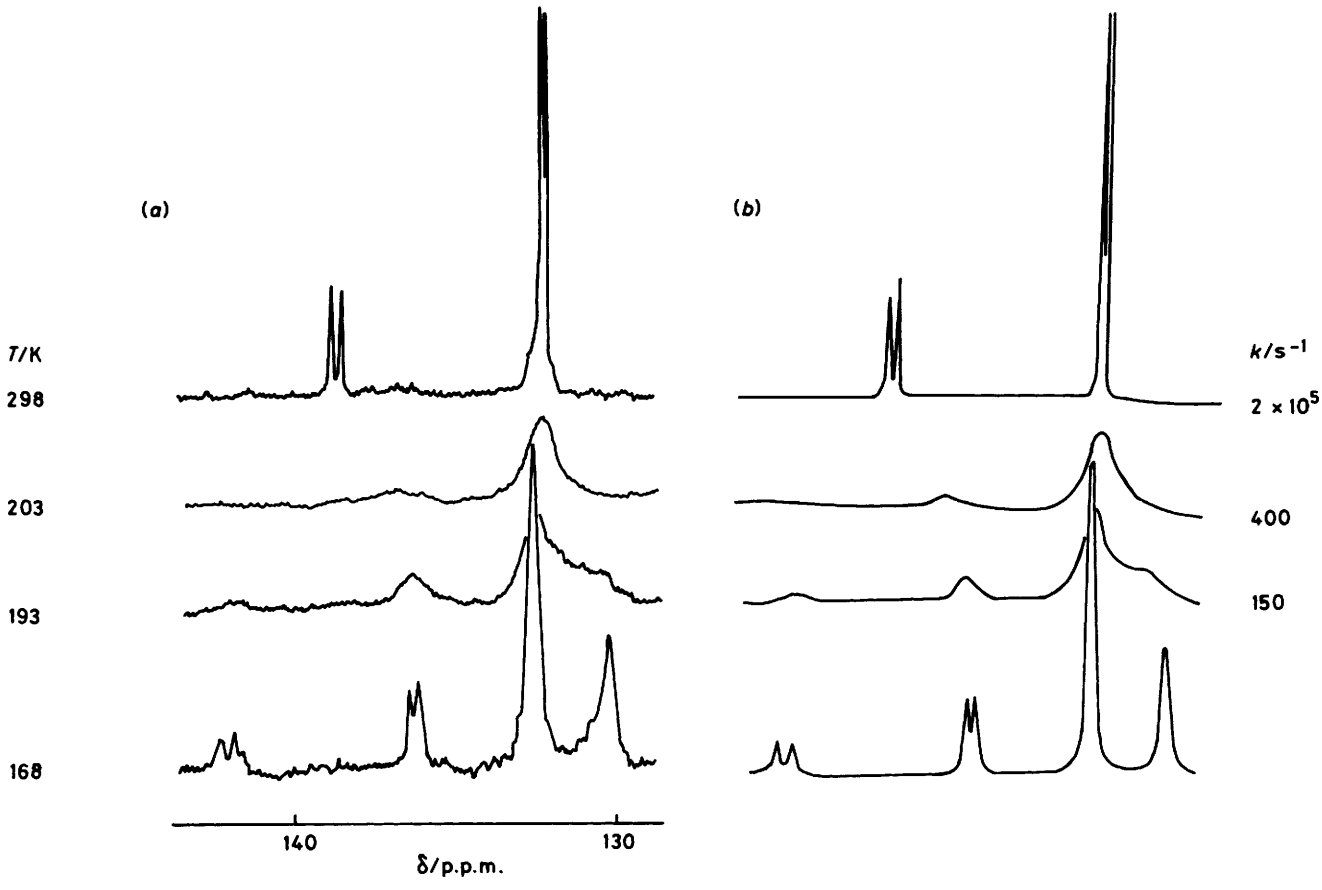

Figure 5. The variable-temperature $^{13}C-\{^1H\}$ triphenylphosphine *ipso*- and *ortho*-carbon subspectra of (2) in CD_2Cl_2: (*a*) observed, (*b*) simulated

the crystal predominates also in solution, then the less intense downfield component of the decoalesced *i*-C signal can be assigned to the unique phenyl ring which is remote from the influence of the co-ordinated arene. The less intense component is upfield for the decoalesced *o*-C and *p*-C signals.

The decoalescence of the signals assigned to the *i*-C and *o*-C atoms was simulated as a two-site exchange problem with superimposed splitting due to ^{31}P coupling. Simulated and observed variable-temperature n.m.r. spectra for these carbons of (2) are illustrated in Figure 5. The rotational barriers, $\Delta G_{200}^{\ddagger}$ (kJ mol^{-1}), obtained for the decoalescence of the *o*-C signals were: (2), 38.4 ± 1.5; (3), 38.2 ± 1.5; (4), 37.7 ± 1.5. These differences for the three alkyl-substituted complexes are insignificant. That no decoalescence was observed in the spectrum of (1) may merely be the result of accidental isochrony, but it is more probably indicative of a substantially lower barrier to rotation about the Cr–P bond.

We ascribe to steric factors the observed increase in the Cr–P

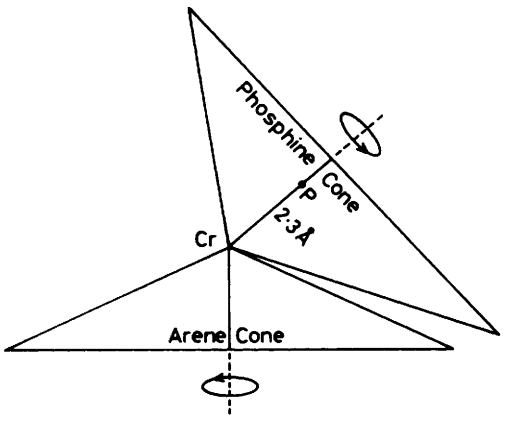

Figure 6. Cross-sectional illustrations of the arene and triphenylphosphine cones of the complexes

rotational barriers for the alkyl substituted complexes. It is also apparent that the major contribution to this arises not from eclipsing of the carbonyl groups by two of the phenyl rings, for which the energy requirement would be similar to that for (**1**), but from passage of one of the phenyl rings past the co-ordinated arene. For this purpose, the co-ordinated arene may be regarded as a disc, rapidly rotating about the chromium–arene bond axis, and whose effective perimeter, relative to the PPh_3 group, is defined by the benzene protons of (**1**), the methyl protons of (**2**), the methylene protons of (**3**), and the α-methylene protons of (**4**).

The steric requirements for the intramolecular rotations for these complexes can be visualized by considering the groups concerned as two cones with a common apex at the centre of the chromium atom; an arene cone, with the rotating co-ordinated arene as its base, and the PPh_3 cone (Figure 6). The cone angle, as originally conceived by Tolman,[5] of PPh_3 is 145° (measured from molecular models).

In the present case, if rotation of the phosphine moiety is assumed to be rapid for (**1**) there will be little interference between the PPh_3 and arene cones. The maximum possible value for the half-cone angle of PPh_3 in (**1**) is thus given by the angle P–Cr–P*, where P* is a point on the projection of the Cr–P bond axis onto the surface of the arene cone. No crystal structure is available for (**1**) but it is a straightforward geometrical exericse, using the known structural parameters of (**3**) and (**4**) and replacing the alkyl groups with hydrogen atoms, to calculate the base diameter of the arene cone. Adopting the standard van der Waals radius of 1.2 Å for a hydrogen atom gives a value for this diameter of 7.3 Å. The calculated P–Cr–P* angle is 70.5°† and the maximum possible cone angle for the PPh_3 ligand in (**1**) is thus 141°. As the Cr–P distance of 2.3 Å is not significantly greater than that defined by Tolman,[5a] we consider that the value of 141° is closely comparable to that generally accepted for this ligand. This lends confidence to our assumption that the observed lack of a decoalescence phenomenon in the spectrum of (**1**) is due to a low barrier to rotation about the Cr–P bond.

As recognised from the outset, regular solid cone angles take no account of the intermeshing of adjacent ligands. A particularly good example of this is the isolable complex $[Pt(PPh_3)_4]$, where without ligand intermeshing it would be impossible to place the four PPh_3 ligands about the metal. Under these circumstance, a bulky phosphine ligand is better described as an 'irregular conic cog'.[6] Even where intermeshing is inappropriate, substantial relaxation of ligand steric demand in a *static* situation may still be achieved by the phosphine adopting an orientation about the metal–phosphorus bond which gives least steric interaction with adjacent ligands. Figures 1 and 2 illustrate that just a situation applies in the solid state for (**3**) and (**4**), and we calculate the base diameter of the arene cone of (**4**) to be 9.3 Å, with P–Cr–P* only 60.5°. However, for (**2**), (**3**), and (**4**) in a rotationally *dynamic* situation, maximum ligand steric demand arises at the least favourable orientation about the Cr–P bond and clearly there is then significant interference between the PPh_3 and arene cones.

† For (**1**) the chromium tilt angle is probably smaller than that found for (**3**) and (**4**), but this should be compensated for by a smaller P–Cr–c(0) angle owing to a reduced interaction between the PPh_3 and co-ordinated benzene compared with hexa-alkylbenzene.

Experimental

Variable-temperature N.M.R. Measurements.—All variable-temperature n.m.r. spectra were recorded at 90.56 MHz (^{13}C) on a Bruker WH360 spectrometer operating in the Fourier transform mode. All n.m.r. samples were filtered under N_2 through a grade 3 glass sinter, freeze–thaw degassed, and sealed in 10-mm (outside diameter) tubes. The temperature of the probe was measured by a thermocouple inserted in an n.m.r. tube filled with toluene to the same depth as the solution in the sample tube. Temperatures are considered accurate to ±2 °C.

Concentrations of the sample solutions were approximately 75 mmol dm^{-3} and all samples were dissolved in CD_2Cl_2. Provided that they were carefully filtered, degassed, and the tube sealed, it was possible to supercool the solutions to at least 20 °C below the nominal freezing point of the solvent CD_2Cl_2, the samples remaining liquid for several hours at these temperatures.

Spectral simulations were performed using the DNMR3 program.[7] Satisfactory fits of simulated to observed spectra were judged by visual comparison. Values of $\Delta G^{\ddagger}$ were calculated using the Eyring equation.

Synthesis.—Hexa-n-propylbenzene. This was prepared by the method of Hopff and Gati.[8] ^{13}C-{^1H} N.m.r. (CD_2Cl_2): δ 136.91 (C_{arene}), 32.23 (CH_2), 25.26 (CH_2), 15.14 (CH_3).

Tricarbonyl(η⁶-hexa-n-propylbenzene)chromium(0). This was prepared by relfuxing $C_6Pr^n_6$ (1.00 g, 3.0 mmol) and $[Cr(CO)_6]$ (0.73 g, 3.3 mmol) in dibutyl ether–tetrahydrofuran (6:1, 35 cm^3) for 1 week. The solvents were stripped off under reduced pressure and unreacted $[Cr(CO)_6]$ removed by sublimation (85 °C at 0.5 Torr). The residue was crystallised from toluene to give yellow-green crystals of $[Cr(\eta^6\text{-}C_6Pr^n_6)(CO)_3]$ (Found: C, 68.4; H, 10.1. Calc. for $C_{27}H_{42}CrO_3$: C, 69.5; H, 9.1%). ^{13}C-{^1H} N.m.r. (CD_2Cl_2): δ 235.79 (CO), 112.38 (C_{arene}), 31.48 (CH_2), 26.85 (CH_2), 14.97 (CH_3).

Dicarbonyl(η⁶-hexa-n-propylbenzene)(triphenylphosphine)-chromium(0), (**4**). This complex was prepared by u.v. irradiation of a freeze–thaw degassed toluene solution of $[Cr(\eta^6\text{-}C_6Pr^n_6)(CO)_3]$ (0.50 g, 1.2 mmol) and PPh_3 (0.34 g, 1.3 mmol). The orange-yellow solution was filtered under N_2, the solvent evaporated and the residue extracted under N_2 with toluene. Slow evaporation of the solvent under N_2 gave orange crystals (0.33 g, 39%) (Found: C, 74.9; H, 8.1. Calc. for $C_{44}H_{57}CrO_2P$: C, 75.3; H, 8.9%).

Crystallography—Crystal data for (**4**). $C_{44}H_{57}CrO_2P$, M = 700.9, crystals obtained as yellow prisms by slow evaporation of a toluene solution are triclinic, space group $P\bar{1}$, a = 13.188(12), b = 13.895(12), c = 11.292(10) Å, α = 90.78(2), β = 107.42(2), γ = 91.97(2)°, U = 1 972.5 Å^3, Z = 2, D_c = 1.18 g cm^{-3}, F(000) = 752, Cu-K_α radiation (λ = 1.5418 Å), μ = 29.9 cm^{-1}.

Intensity data were collected from a crystal of dimensions

Table 3. Atomic co-ordinates for the non-hydrogen atoms of (**4**)

Atom	*x*	*y*	*z*	Atom	*x*	*y*	*z*
Cr	0.349 5(1)	0.195 6(1)	0.122 4(1)	C(52)	0.240 6(6)	−0.110 5(4)	−0.056 5(8)
C(1)	0.198 3(5)	0.166 3(4)	0.174 4(6)	C(53)	0.283 5(8)	−0.209 6(5)	−0.039 1(9)
C(2)	0.176 2(5)	0.236 3(4)	0.076 9(7)	C(61)	0.259 7(5)	0.000 6(5)	0.260 5(7)
C(3)	0.200 5(5)	0.218 3(4)	−0.033 7(7)	C(62)	0.183 1(6)	−0.084 8(5)	0.230 3(8)
C(4)	0.245 2(5)	0.129 2(4)	−0.050 3(6)	C(63)	0.208 4(8)	−0.152 1(6)	0.344 4(8)
C(5)	0.267 2(5)	0.059 1(4)	0.044 8(7)	P	0.426 7(1)	0.301 3(1)	0.286 4(2)
C(6)	0.240 8(5)	0.077 0(4)	0.157 5(6)	CP(11)	0.565 0(5)	0.342 7(5)	0.302 4(7)
C(7)	0.467 1(5)	0.122 8(5)	0.176 6(6)	CP(12)	0.644 1(6)	0.278 6(6)	0.350 2(8)
O(1)	0.539 1(4)	0.072 2(4)	0.205 3(5)	CP(13)	0.751 5(5)	0.305 1(6)	0.367 8(8)
C(8)	0.415 9(5)	0.265 9(5)	0.030 9(8)	CP(14)	0.775 4(7)	0.392 2(7)	0.334 2(9)
O(2)	0.456 7(5)	0.309 6(4)	−0.029 7(6)	CP(15)	0.698 9(8)	0.456 0(7)	0.284 3(11)
C(11)	0.167 6(5)	0.186 3(5)	0.289 4(7)	CP(16)	0.592 4(6)	0.431 2(6)	0.268 5(9)
C(12)	0.067 6(6)	0.132 2(6)	0.293 7(8)	CP(21)	0.356 8(5)	0.414 7(5)	0.277 8(8)
C(13)	0.016 2(8)	0.182 1(7)	0.382 9(10)	CP(22)	0.343 3(6)	0.468 5(5)	0.167 2(9)
C(21)	0.123 8(5)	0.330 5(5)	0.091 6(7)	CP(23)	0.286 2(7)	0.553 0(5)	0.146 2(10)
C(22)	0.003 0(5)	0.318 8(6)	0.077 8(8)	CP(24)	0.241 5(8)	0.582 6(6)	0.237 5(13)
C(23)	−0.035 3(7)	0.408 5(6)	0.120 3(9)	CP(25)	0.249 7(8)	0.530 3(8)	0.340 9(12)
C(31)	0.181 3(6)	0.292 6(5)	−0.139 2(7)	CP(26)	0.309 1(6)	0.445 8(6)	0.365 0(8)
C(32)	0.065 1(6)	0.298 4(5)	−0.216 1(7)	CP(31)	0.450 4(5)	0.261 0(5)	0.447 0(7)
C(33)	0.050 2(8)	0.361 5(6)	−0.330 0(8)	CP(32)	0.440 7(5)	0.163 2(5)	0.467 5(8)
C(41)	0.269 7(5)	0.105 2(5)	−0.171 6(7)	CP(33)	0.459 1(6)	0.127 2(6)	0.588 9(8)
C(42)	0.169 3(6)	0.072 3(5)	−0.277 1(7)	CP(34)	0.487 3(6)	0.191 7(7)	0.687 3(8)
C(43)	0.197 2(8)	0.025 3(7)	−0.385 0(8)	CP(35)	0.501 4(6)	0.287 3(7)	0.668 9(9)
C(51)	0.316 0(5)	−0.036 2(4)	0.029 7(7)	CP(36)	0.483 7(6)	0.324 4(6)	0.551 3(8)

0.16 × 0.17 × 0.46 mm mounted on *c* (reciprocal lattice layers 0—7) and from a second crystal of dimensions 0.19 × 0.39 × 0.42 mm mounted in turn on [110] (layers 0—2) and on *a* (layers 0—3). Equi-inclination multi-film Weissenberg exposures were scanned by use of a microdensitometer (S.E.R.C. Service, Daresbury Laboratory). The merging *R* index was 0.057 for 2 575 unique data (no absorption correction). Approximate co-ordinates for the Cr and P atoms were obtained from a Patterson synthesis, and the C and O atoms were located in difference syntheses alternating with cycles of refinement. The hydrogen atoms were included as 'riding' atoms at calculated positions in the last cycles. Refinement converged at *R* 0.059, $R'[=(\Sigma w\Delta^2/\Sigma wF^2)^{\frac{1}{2}}]$ 0.088: blocked-matrix least-squares refinment, all non-hydrogen atoms anisotropic, 433 parameters, weights in last cycle given by $w = [1 + 0.0070 F^2]^{-1}$. The final difference synthesis (max. deviations from planarity, +0.38, −0.51 e Å^{-3}) showed no indications of disorder or of the presence of lattice solvent molecules. The SHELX 76 program system[9] was used in all calculations. Atomic co-ordinates are given in Table 3.

Acknowledgements

We thank Dr. D. Reed of the S.E.R.C. High-field NMR Facility at the University of Edinburgh for obtaining the 90.56-MHz ^{13}C n.m.r. spectra, Miss Stella Denholm for experimental assistance, Professor Kurt Mislow for helpful discussion, and the N.A.T.O. Scientific Affairs Division and the U.S. National Science Foundation for financial support.

References

1 (*a*) G. Hunter, T. J. R. Weakley, K. Mislow, and M. G. Wong, *J. Chem. Soc., Dalton Trans.*, 1986, 577; (*b*) D. J. Iverson, G. Hunter, J. F. Blount, J. R. Damewood, jun., and K. Mislow, *J. Am. Chem. Soc.*, 1981, **103**, 6073; (*c*) G. Hunter, J. F. Blount, J. R. Damewood, jun., D. J. Iverson, and K. Mislow, *Organometallics*, 1982, **1**, 448.
2 M. A. Bennett, R. N. Johnson, and T. W. Turney, *Inorg. Chem.*, 1976, **15**, 111; J. B. Docherty, D. S. Rycroft, D. W. A. Sharp, and G. A. Webb, *J. Chem. Soc., Chem. Commun.*, 1979, 336; W. D. Jones and F. J. Feher, *Inorg. Chem.*, 1984, **23**, 2376; C. Bushweller, C. Hackett, S. Hoogusian, A. D. English, and J. S. Miller, *ibid.*, 1981, **20**, 3448; J. A. Brunelle, C. H. Bushweller, and A. D. English, *J. Phys. Chem.*, 1976, **80**, 2598; C. H. Bushweller, C. D. Rithner, and D. J. Butcher, *Inorg. Chem.*, 1986, **25**, 1610.
3 J. W. Fuller and B. V. Johnson, *J. Organomet. Chem.*, 1975, **96**, 99.
4 H. C. Clark, *Isr. J. Chem.*, 1976, **15**, 210.
5 (*a*) C. A. Tolman, *J. Am. Chem. Soc.*, 1970, **92**, 2956; (*b*) C. A. Tolman, W. C. Seidel, and L. W. Gosser, *ibid.*, 1974, **96**, 53; (*c*) C. A. Tolman, *Chem. Rev.*, 1977, **77**, 313.
6 G. Ferguson, P. J. Roberts, E. C. Alyea, and M. Kahn, *Inorg. Chem.*, 1978, **17**, 2695.
7 G. Binsch and D. A. Kleier, Quantum Chemistry Program Exchange, Indiana University, 1970, vol. 11, no. 165.
8 H. Hopff and A. Gati, *Helv. Chim. Acta*, 1965, **48**, 509.
9 G. M. Sheldrick, SHELX 76 Program for Crystal Structure Determination, University of Cambridge, 1976.

Received 24*th July* 1986; *Paper* 6/1511